UC Santa Cruz
UC Santa Cruz Electronic Theses and Dissertations

Title
Detection of Biomolecules on a Nanopore-Microfluidic Platform

Permalink
https://escholarship.org/uc/item/7tr40179

Author
Li, Yucheng

Publication Date
2019

Copyright Information

Peer reviewed|Thesis/dissertation

UNIVERSITY OF CALIFORNIA

SANTA CRUZ

**DETECTION OF BIOMOLECULES ON A NANOPORE-MICROFLUIDIC
PLATFORM**

A thesis submitted in partial satisfaction

of the requirements for the degree of

MASTER OF SCIENCE

in

ELECTRICAL ENGINEERING

by

Yucheng Li

June 2019

The Thesis of Yucheng Li

is approved:

_____
Professor Holger Schmidt, Chair

_____
Professor Nobuhiko Kobayashi

_____
Professor Marco Rolandi

_____
Lori Kletzer

Vice Provost and Dean of Graduate Studies

Table of Contents

List of Figures

Abstract

DETECTION OF BIOMOLECULES ON A NANOPORE-MICROFLUIDIC PLATFORM

by

Yucheng Li

In this work, we combined the micropore fabrication process into the fabrication processes of the microfluidic device. With certain post-treatment processes, we integrated solid-state nanopore with the microfluidic chip and created a nanopore-microfluidic platform. On this platform, we demonstrated the first detection of NaCMC (Sodium Carboxymethyl Cellulose) with a nanopore. Based on the demonstration of nucleic acids and NaCMC detection separately on this platform, we successfully demonstrated the multiplex detection in the mixture of NaCMC and λ-DNA. With the combination of feedback controlled gated system, we also demonstrated a controlled number of NaCMC delivery on this platform. In order to improve the solid-state nanopore sensitivity in the nanopore-microfluidic platform, we successfully performed ion-sculpting on the direct drilling nanopores. Electrical properties of the ion-sculpted nanopore have been investigated preliminarily, and NaCMC detection on the ion-sculpted nanopore has been demonstrated.

Acknowledgements

1 Introduction

1.1 Nanopore

A nanopore is an opening on the membrane, the diameter of which is in the level of 1-100 nm. The membrane where the nanopore sits is usually electrical insulating. When both sides of the membrane are filled with electrolytic, and there is an electrical potential difference between two sides of the membrane, there will be an electrical current through the nanopore. Because the diameter is close to the size of biomolecules, if the biomolecules are passing through the nanopore, the current change will be detectable, which makes nanopore an ideal candidate of single molecule detector.

There have been a lot of researches of nanopore about the properties as well as the application of nanopore. Siwy et al.[1] discussed diode-like current response of cone nanopore. Smeets et al.[2] discussed the low-frequency noise of solid-state nanopore. Zhang et al.[3] demonstrated using nanopore as an electrode in the electrochemistry system. Chen et al.[4] demonstrated detecting single DNA molecule transport with the nanopore. Nanopores also have the capability of detecting nucleic acid with single nucleotide precision[5,6], which leads to one of the most important applications of nanopore-nuclear acid sequencing. After three decades, some commercial products of nanopore sequencing have already been available.[7]

Based on the different materials of the nanopore membrane, there are two categories of nanopore, solid-state and biological nanopore. Figure1 shows the samples of the

structure of biological nanopore and solid-state nanopore. In the 1.1.1 and 1.1.2, these

two kinds of nanopore will be introduced.
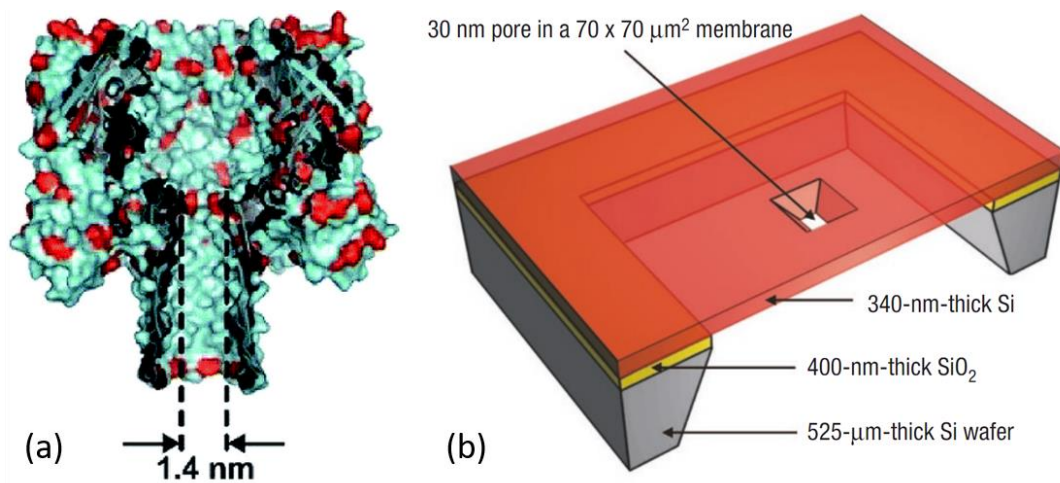
Figure 1. a. biological nanopore[8] b. solid-state nanopore[9]

1.1.1 biological nanopore

A biological nanopore is the nanopore built with proteins. Some cells have proteins

which form transmembrane channels/pores to allow ions and solution to pass. The

diameter of these pores is around 1 to 2 nm, which means the pores formed in these

proteins are nanopores. In nanopore experiments, the protein is often inserted in a free-

standing lipid layers to form a nanopore spontaneously[10] and DNA, and RNA can go

through the proteins and be detected.[11,12] There are two kinds of proteins which are

usually used as biological nanopores, α-haemolysin which is a protein secreted by

Staphylococcus aureus[13] and Mycobacterium smegmatis porin A (MspA) which is a

protein forming the channel for hydrophilic solutions in M. smegmatis [11].

2

1.1.2 solid-state nanopore

A solid-state nanopore is the pore built on solid-state membranes. Solid-state has been built on different materials, for example, silicon[14], silicon oxide[9], silicon nitride[15], Al_2O_3[16], and graphene[17–19], as well as different methods, for example, electron beam tuning[9], feedback chemical etching[14], and ion beam sculpting[15].

Compared to biological nanopores, solid-state nanopore has many advantages. First, because the nanopore is fabricated using solid-state materials like SiO_2 or silicon nitride, they are more stable and have a much longer lifetime compared to biological nanopore proteins. And because of the lifetime, solid-state nanopore can be reused for several times. Second, it is easier for solid-state nanopore to integrate with other platforms. Third, because the solid-state nanopore is manually fabricated compared to the biological nanopore which is got from cells, the diameter of the nanopore can be controlled to detect different kinds of biomolecules especially the molecules like a virus which is much larger than biological nanopore. Last but not the least, the experiment circumstance like temperature and pH doesn't need to be that strict. Solid-state nanopore has the potential to work in extreme environments like outer space.

1.2 Microfluidic platform

Microfluidics is the technology to manipulate fluidics in micrometer level channels.[20] Researchers and engineers have already developed a lot of applications in many areas including biology researches and public health like cell sorting platform and point-of-care diagnosis devices.[21,22] Microfluidics give people the possibility to process many

kinds of measurements and reactions with very little sample, which has realistic meanings in real-world case when it may be hard to get a high concentration sample.

1.2.1 Integration of microfluidic device and nanopore

Besides the components for fluidic samples introducing, combining and mixing, detectors are also an important part on the microfluidic platform because many applications like diagnostics are related to test biological samples and detect different kinds of molecules. Because nanopore is also designed from single level molecule detection and the dimension of the nanopore is close to the micrometer fluidic channel, it is normal that people have tried to combine nanopores on preexisting microfluidic platforms. Jain et al. [23] demonstrated the method of using transfer printing to integrate microfluidics channel with solid-state nanopore and demonstrated single DNA detection using this platform. In our group, we have already developed a kind of optofluidic chip integrated with nanopores and demonstrated different applications on this platform. Rudenko et al. [24] demonstrated detecting ribosome and viruses; Liu et al. [25] demonstrated electro-optical detection of biomolecules based on the optofluidic-nanopore platform.

2 Multiplexed and Gated Detection of Biomolecules with Solid-state Nanopore

2.1 Fabrication methods of a microfluidic device with pre-fabricated micropore

The mechanism of molecule detection using nanopore is based on measuring the ionic current change when molecules are passing through a nanopore. When a voltage is applied across the nanopore, the electrolytic solution filled in the nanopore as well as around the nanopore will be driven and form a measurable ionic current. If there are also molecules like nuclear acid and proteins in the electrolytic solution which carry certain amount charges, they will also be driven by the electrical field in the electrolytic solution and passing through the nanopore. With an applied voltage across the nanopore which is around several hundred millivolts to several volts, the current level is usually in nA or even pA level. In this case, for precise current measurement, people usually use a patch clamp system to measure the current through the nanopore. Furthermore, because those molecules can partially block the electrolytic solution's ions, as well as they carry different amounts of charges from the ions when they are passing through the nanopore, there will be a current change pulse, either a dip or a peak, which indicates this translocation event of the molecule. Depending on the difference of the size and the charges per unit length on different molecules, the amplitude and the duration of this pulse will be different. As a result, if we analyze

these pulses, we can get the information of molecules in the electrolyte like the structure and the charge distribution of these molecules.

Previously in our group, we used focused ion beam (FIB) to fabricate nanopore on an optofluidic chip. Firstly, we drilled an around 5μm by 5μm square on top of the chip as the micropore. In this step, we removed most of the oxide layer on top of the liquid core channel to leave a thin membrane. Then we reduced the current and exposed time of the ion beam and drilled the nanopore on the leftover membrane. However, a shortcoming exists in this method. The thickness of the leftover membrane, which is equivalent to the length of the nanopore, is difficult to be controlled or measured. This will cause difficulty to predict the amplitude and the duration time of the current change. This non-predictability also means that, since we need to drill micropore every time, the nanopore membrane properties are not consistent, and because of the edge effect of FIB drilling, the thickness of different positions of one membrane are not consistent. The center of the membrane is usually thicker, which means the length of the nanopore is longer than expected, which reduce the sensitivity of nanopore.[26]

For the goal of a more controlled process, our collaborator Professor Aaron Hawkins and his group have been developing a new fabrication process of microfluidic chips integrated with a micropore on a ~100 nm thick SiO_2 membrane centered the hollow core channel. With this pre-fabricated membrane, not only we can have a better approximation of current spike amplitude and duration, but also, we can have more precise nanopore drilling with this thin and known thickness membrane.
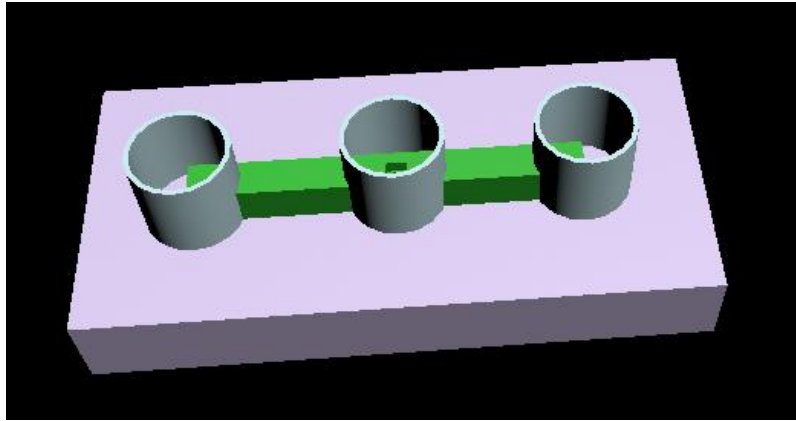
Figure 2. Schematic of the microfluidic chip integrated with a solid-state nanopore

The schematic of the device is shown in Figure 2. The green cuboid stands for the hollow core channel on the chip, and the azury hollow cylinders stand for the three reservoirs we have on the chip which are on top of the inlet, the nanopore and the outlet of the channel separately. The process steps are as follows, as illustrated in Figure 3. And the fabrication processes are described below.

The method to fabricate a membrane on top of the hollow core channel with known thickness is to set a stop-etch layer to tune the chemical etch process. Here we use amorphous silicon as this stop-etch layer. In Figure3, inset (a) shows the <100> oriented, 100mm diameter silicon substrate we used. Inset (b) shows that an approximately 1 cm long SU8 line is patterned on the substrate. The area of the cross-section of this line is 12μm x 5μm. SU8 is the sacrificial material in the process, and the position occupied is the microfluid hollow core channel later. Inset (c) stands for the process of deposition of a 100 nm SiO_2 using Plasma Enhanced Chemical Vapor Deposition (PECVD). We also use PECVD to deposit a 30 nm thick amorphous silicon

layer and then 100 nm SiO_2 layer in the inset (d) (step 4) and deposit a 5μm thick SiO_2 layer in the inset (e) (step 5). Inlet and outlet are formed in the thick 5μm SiO_2 layer through a lithography process and HF wet etching afterward. After the underlying SU8 core gets exposed, it is removed by piranha (sulfuric acid and hydrogen peroxide), and we get the hollow core channel. Also, by using a lithography step followed by HF wet etching over the amorphous silicon stop-etch layer, we get the micropore. And the membrane of the micropore should be the 100 nm SiO_2 layer we deposit in the inset (d) (step 4).
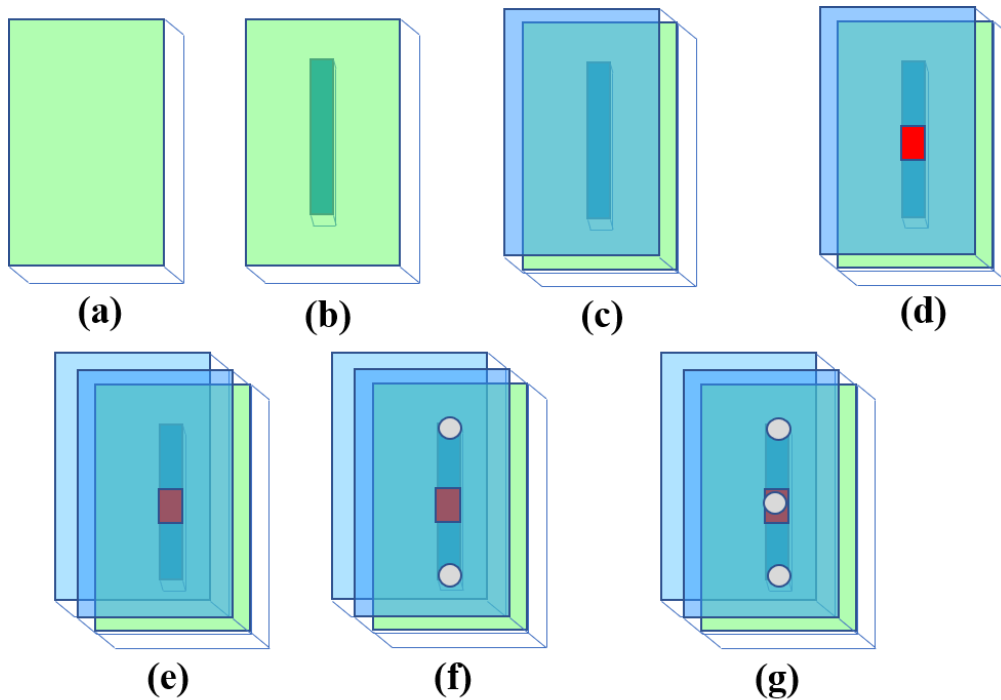
Figure 3. Outline of process steps used for the fabrication of chips containing micropores and membranes suitable for nanopore FIB drilling.

Ideally, we should get only 100nm SiO_2 layer left on top of the hollow core layer. But in the real fabrication process, some of the chips have much thicker membrane than

expected on top of the channel. Here is the SEM photo of the intersection of one of the micropore fabricated via the process mentioned above.
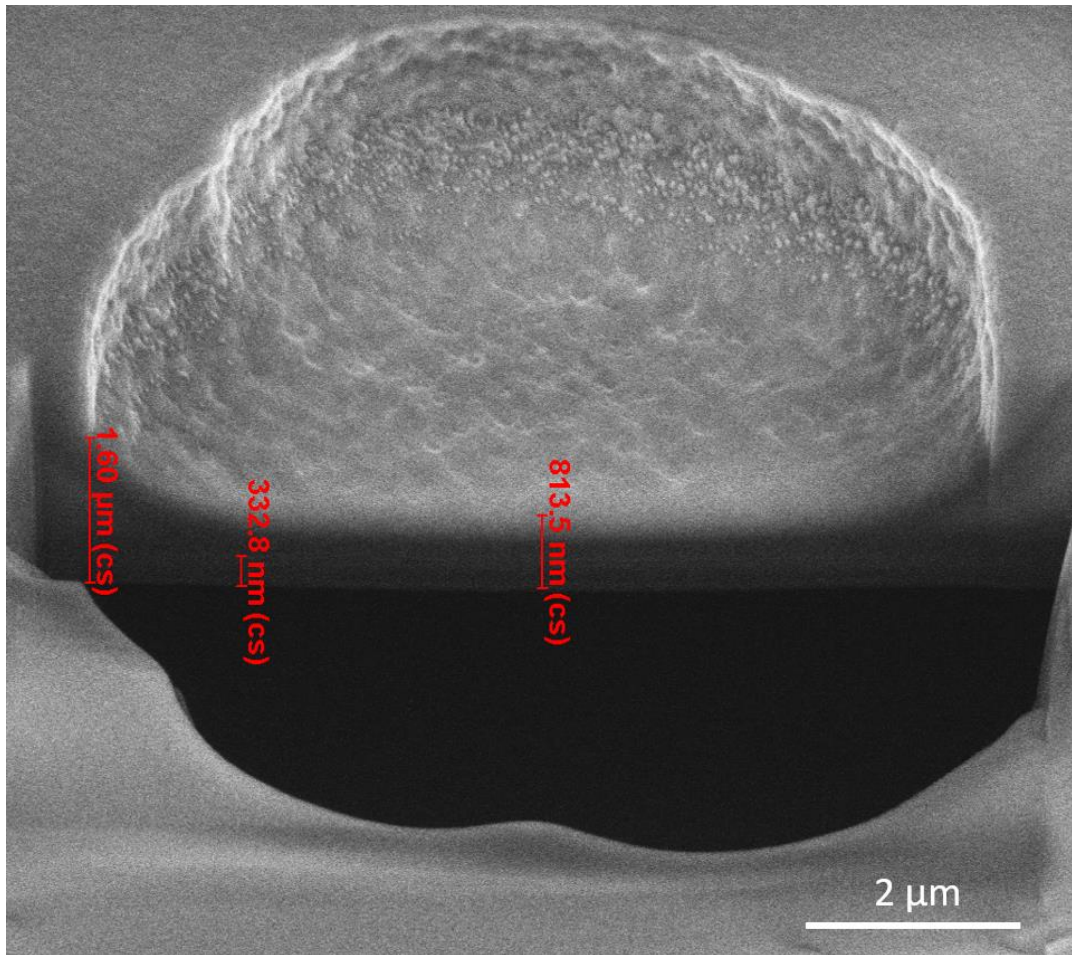
Figure 4. SEM image of the cross-section of a prefabricated micropore membrane

From the measurement bars given by the SEM in the picture, we can know that the edge of the membrane is over 1.5µm thick, and the bottom of the membrane is around

800nm thick. The shape of the micropore should be like a cylinder, but the membrane thickness is not consistent on the surface of the micropore, and it looks like a bowl. We can also tell that the surface of this micropore is not smooth. The photo gives us a hint that after the etch process, the membrane is not etched all the way to the stop layer. That may be because the etch time is not enough. In the future, we need to study more about the etch process, and the etch time. However, this new process still gives us a flat membrane in the small area of the center of the micropore. So, we can measure the thickness of the center of the membrane and thin down the membrane accordingly to get a new micropore with a thinner membrane. From the thinning process, we can also know approximately the thickness of this new membrane. The process in details is described below. Firstly, we thin down a small square near the center of the pre-fabricated micropore and keep exposing the ion beam until it drills all way through the micropore membrane. Then we measure the membrane thickness on the cross-section of this test square. Then we put the measurement scale bar on the screen and then turn to the position we want to get the real thin membrane (which is usually at the center). Then we start to thin down the micropore membrane and then we use the scale bar to know how thick we should drill and when to stop. Then we can drill the nanopore on that new membrane. Finally, we deposit some silicon oxide on the test hole to seal it.

Figure 5 and Figure 6 are the pictures of thinning down the process and the picture of the thinner membrane and nanopore photo.
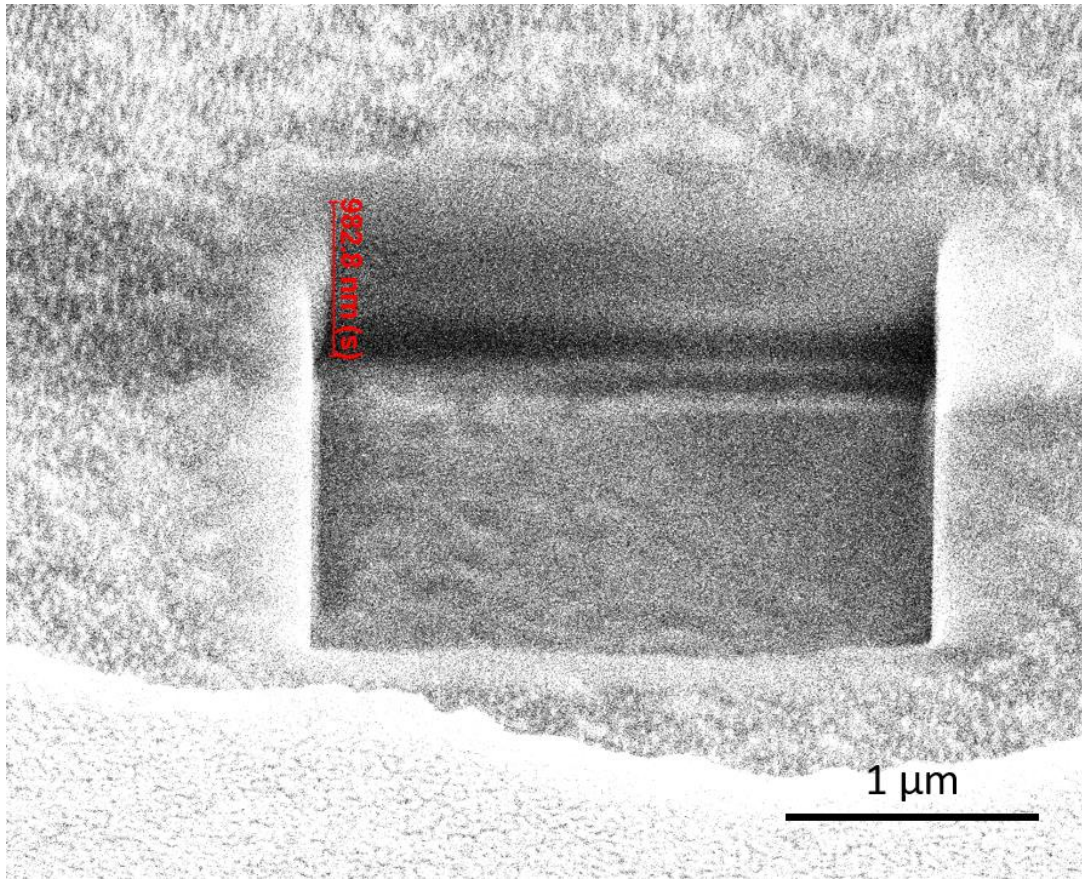
Figure 5. SEM image of the thinning down process on the pre-fabricated micropore membrane
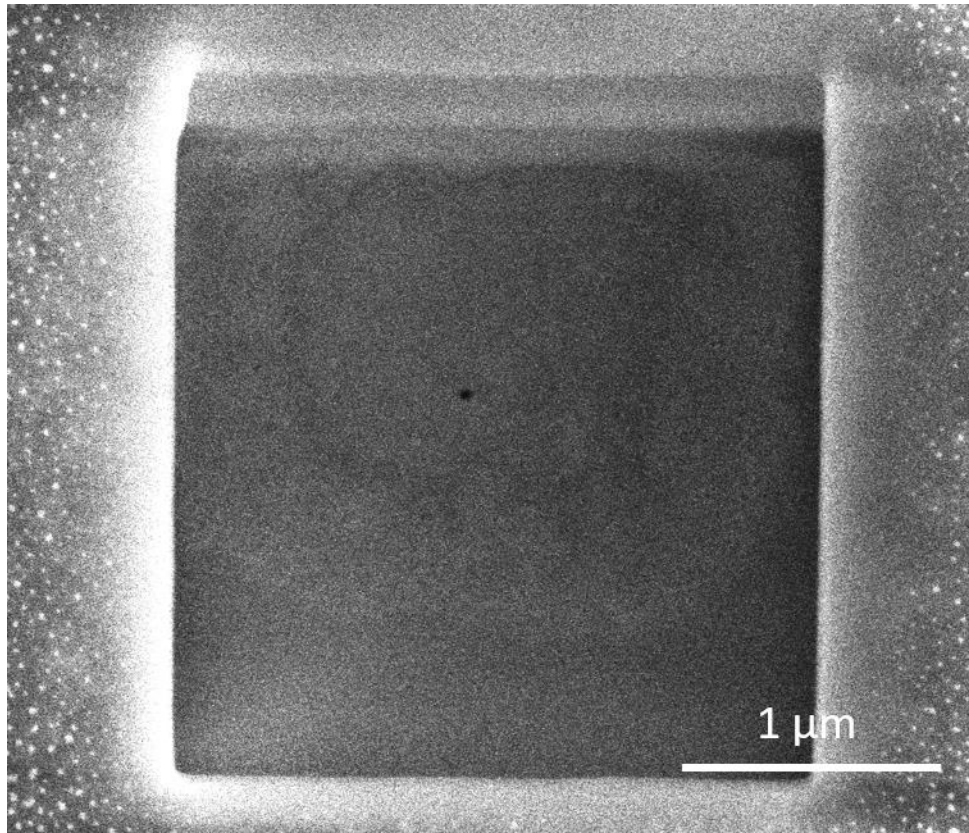
Figure 6. SEM image of a nanopore and micropore fabricated on a prefabricated micropore membrane

2.2 Nanopore fabrication method

The nanopore on our device is fabricated by direct drilling. We use focused ion (Ga+) beam (FIB) to drill our nanopore. The system we use is FEI Quanta 3D Dual Beam.

As it is discussed in 2.1, before drilling nanopores, we need to thin down the oxide layer on top of the liquid core and finally get a thin membrane. The need to get a thin membrane is that because of the limitation of the focus of ion beam, it is hard to drill through a thick membrane and get a small nanopore simultaneously. So, we need to

make the thickness of the membrane small enough to ensure the nanopore drilled afterward will be through.

There are two parameters to tune the FIB system to control the diameter of nanopore we drill. One is ion current. With smaller current smaller pore is supposed to get when other parameters don't change. This parameter can be changed in the control panel of FIB. Another parameter is the ion beam exposure time. With shorter exposure time, fewer ions will hit the membrane, and it is supposed to get a smaller nanopore. For a nanopore with a diameter around 20 nm, the exposure time is usually around 1 second. It is nearly impossible for a human to response that fast to turn on and turn off the ion beam in that short time. So, for precise process control, we use nanometer pattern generation system (NPGS) to control the ion beam exposure time on FIB.
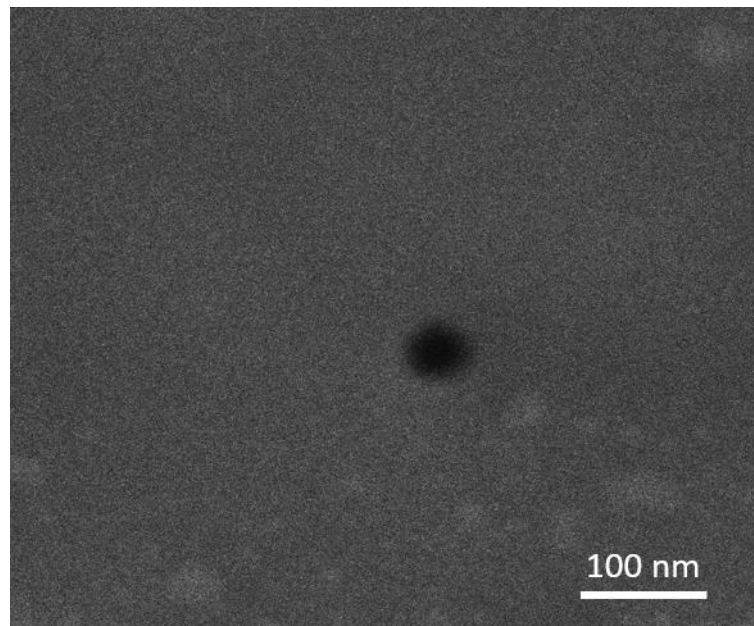
Figure 7. SEM image of a nanopore fabricated in a single device

NPGS is an SEM lithography system. Combined with FEI Quanta 3D FEG dual (SEM/FIB) system, we can fabricate certain pattern with the control of exposing time and position. In our case of fabricating single nanopore, we set the time of exposure in the NPGS. For the further application, we can also import CAD to design nanopore arrays on a single membrane. The way to achieve this is to design a CAD with the information of nanopores position and distance between the first pore and the second pore. One thing needed to take care is that the distance predetermined in the CAD design is dependent on certain magnification ratio. If the magnification ratio when drilling the nanopore is not the value in your CAD design, you may not get the expected nanopore arrangement.

The below picture shows one of the examples of multiple nanopores drilling simultaneously. Fig. 8a shows the SEM photo of the membrane with two nanopores. And inset (b) and (c) shows the picture of the two nanopores separately.
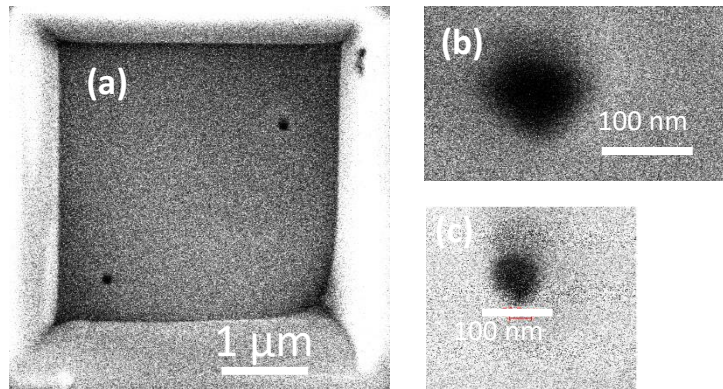
Figure 8. a. SEM image of two nanopores fabricated in a single device; b. Zoomed in image of bigger nanopore (~50nm); c. Zoomed in image of smaller nanopore (~30nm).

2.3 Sodium Carboxymethyl Cellulose (NaCMC) detection

Cellulose is a type of linear polymer which is the main component of the primary cell wall of green plants and vegetable fiber. It is widely used in industry and also has some specific potential and capability in medical and biochemistry research. Besides the usage of bulk cellulose, its single molecule level detection is also necessary for some of the interest. Especially in astrobiology, cellulose has already become a promising target to detect in searching the evidence of life on other planets.[27] For this purpose, the capability to detect cellulose in single molecule level becomes more and more important.

We use our microfluidic devices combined with solid-state nanopore, which has very strong capability to detect biomolecules in single molecule level to perform cellulose detection experiments. In our experiment, NaCMC (Sodium Carboxymethyl Cellulose, average Mw ~90,000) as the sodium salt of a kind of cellulose derivatives, Carboxymethyl Cellulose was selected as the target molecule to detect using a ~20nm nanopore (Fig 9a). For the preliminary experiment, we set the concentration of NaCMC solution as 2.5wt%. The diameter of each NaCMC single rod-like molecule is 0.68nm. [28] The buffer we choose to use 1XT50, which is the same buffer we used for λ-DNA. The reason to choose this buffer is that about the mixture detection experiments discussed next unit, we need to mix the solution of NaCMC and λ-DNA. In that case, they need to sit in the same buffer.

Translocation of NaCMC molecules was seen when a voltage of 10V was applied across the nanopore and outlet reservoir. Part of the current trace of the molecular

translocation events is shown in Fig 9b, and a zoomed in translocation event is depicted in Fig 9c. The amplitude of each translocation is around 300pA, which is obviously distinguishable compared to the random noise with around 50pA amplitude. A scatter plot of dwell time and differential current of individual translocation events are plotted which is shown in Fig 9d. The average dwell time of the translocation events is found to be 0.499ms, whereas the average differential current amplitude is 308.48pA.

From the above results, we can claim that we are able to detect NaCMC molecules through our solid-state nanopore.
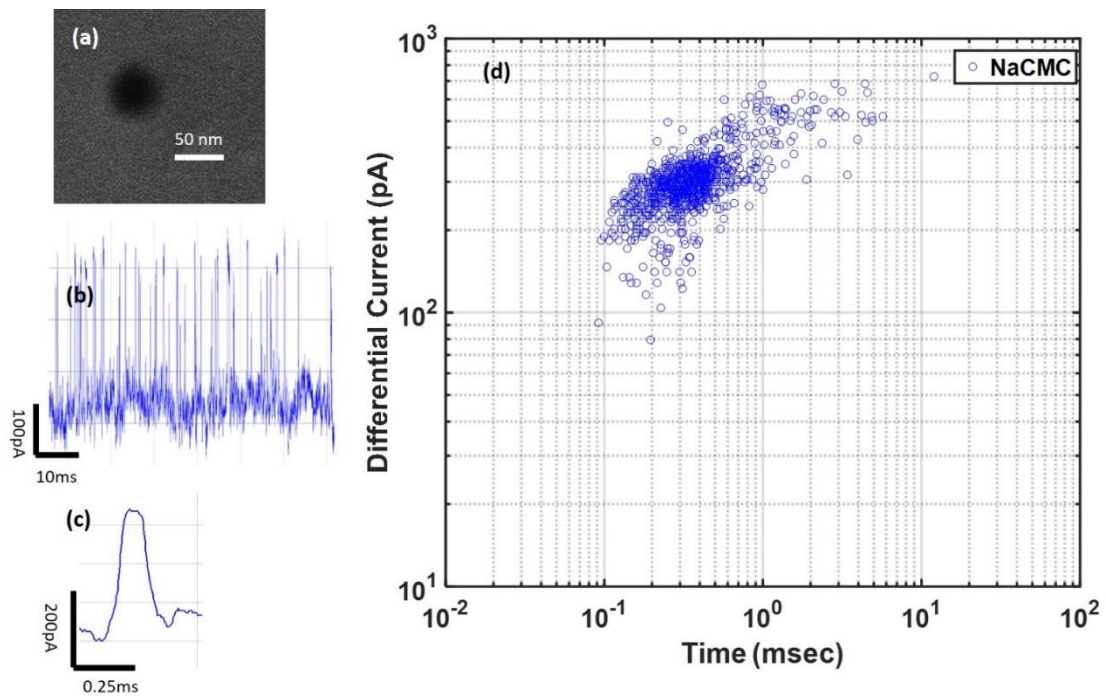
Figure 9.a. SEM image of the nanopore used to detect NaCMC molecules; b. Current trace of NaCMC translocation events; c. Zoomed in single NaCMC translocation; d. Scatter plot of dwell time vs. differential current of NaCMC translocations.

2.4 Nucleic Acid Detection

The nucleic acid is the found part of life genetic information. The single molecule level of nuclear acid is extremely vital in multiple areas like genetic tests, disease diagnosis, and even in the process to detect life in outer space. Nucleotides on the nucleic acid strings carry charges, which means they can be dragged by the electrical field, which means the possibility to detect them using solid-state nanopore.

2.4.1 λ-DNA detection

Previously, we have demonstrated different biomolecular detection using nanopore. However, the detections were done in different devices using different nanopores. As a part of continuous development and a more pragmatic approach, multiplexed detection of different biomolecules using the same nanopore is the next obvious step. To achieve multiplexed detection, λ-DNA molecules were selected as a second target and loaded in the same nanopore (Fig. 9a), which was used to detect NaCMC molecules. Translocation events were seen at a voltage of 10V across the nanopore and outlet reservoir, as shown in Fig. 10a and b. A scatter plot of dwell time and differential current of all translocation events is plotted in Fig 10c. The concentration we used in this experiment is 3×10^{12}/mL. The average amplitude of current modulation and dwell time is found to be 30.35nA and 0.341ms respectively.
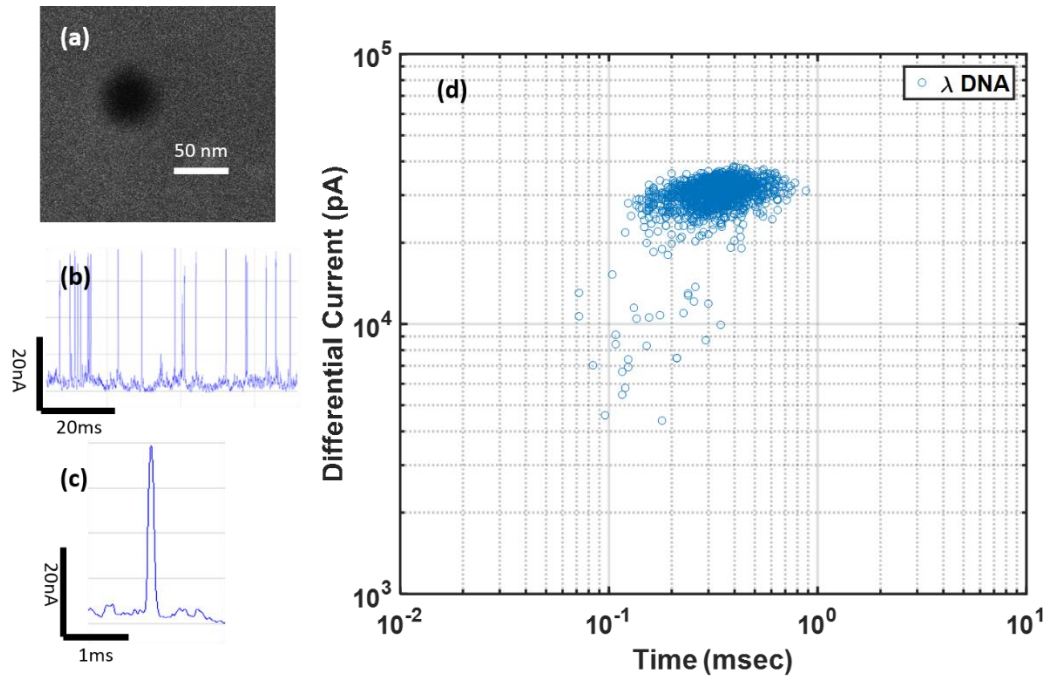
Figure 10. a. SEM image of the nanopore used to detect λ-DNA (same as Figure9a) b. Current trace of λ-DNA translocation events; c. Zoomed in single λ-DNA translocation; d. Scatter plot of dwell time vs differential current of λ-DNA translocations.

2.4.2 DNA Ladder detection

DNA Ladder is a commercial product which is a mixture of multiple kinds of DNA segments with known molecular size and it is often used to estimate DNA size by agarose gel electrophoresis. The DNA ladder we used in our experiments is from Thermo Fisher (100bp DNA Ladder). It includes 13 kinds of DNA segments with different length range from 100 base pairs to 2000 base pairs. (Each base pair is 0.34 nm long approximately. [29])The concentrations of 13 kinds of DNA segments are from around 2×10^{13} /mL to around 3×10^{14}/mL. In our experiments, we diluted the original DNA ladder solution 100 times and loaded them into our device.

The SEM picture of the nanopore is shown in Fig. 11a. The current trace of the translocation events generated by the DNA segments are displayed in Fig.11b, and a zoomed in view of an individual current trace is shown in Fig. 11c. The scatter plot of dwell time and differential current of each individual translocation events are shown as Fig. 11d. Barely three subgroups are seen in the scatter plot, indicating the possibility to distinguish different length DNA segments using single nanopore in the future.
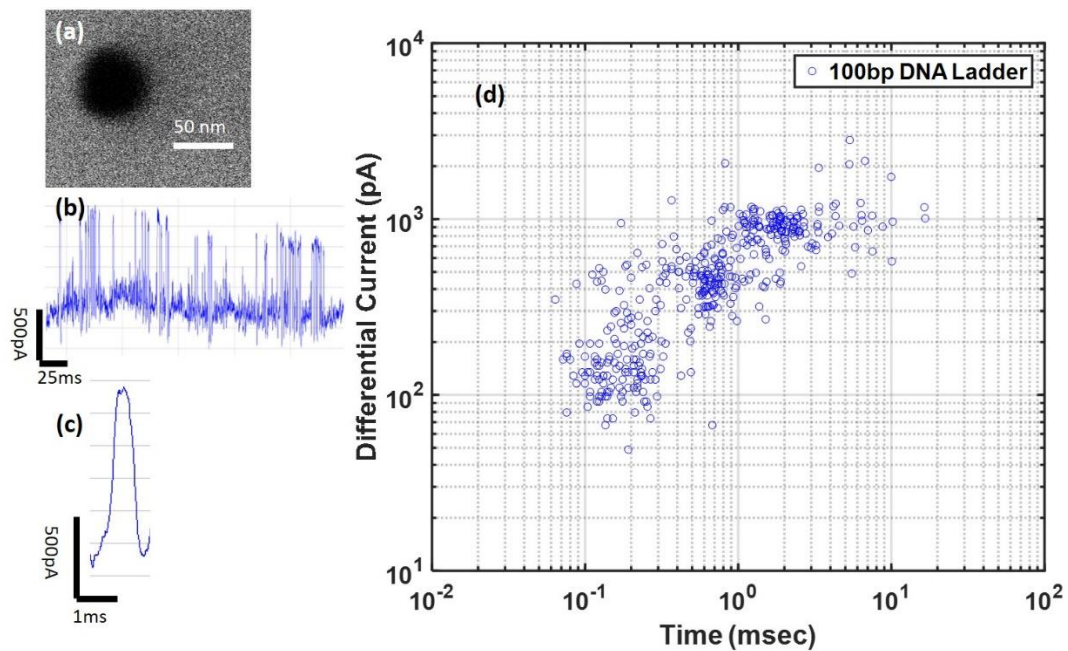
Figure 11. a. SEM image of the nanopore used to detect 100bp DNA Ladder; b. Current trace of 100bp DNA Ladder translocation events; c. Zoomed in single 100bp DNA Ladder translocation; d. Scatter plot of dwell time vs. differential current of 100bp DNA Ladder translocation

2.5 Multiplex detection of a particle mixture

Multiplex molecules detection has very realistic applications in the real world. For example, in the diagnostics area, samples from the human body like urine and blood always include multiple bioparticles. If the platform can distinguish them and get the

19

information of existence or even the concentration of all kinds of bioparticles, that will be very helpful for diagnosis. From our previous research, we can see that due to the different diameter of molecules as well as the different charges carried by different kinds of molecules, when one molecule coming through the nanopore, it will create different current spike pattern. We can determine the kind of each molecule by identifying this spike amplitude and duration and compare to the spike patterns collected previously on this device. Microfluidic channel with solid-state nanopore has the potential to distinguish multiple particles in a mixture of them.

From the previous experiments, we have already detected NaCMC and λ-DNA molecules using the same nanopore. From the properties of these two molecules, we can predict that λ-DNAs have higher charge compared to NaCMC molecules and it is expected to have a higher current modulation amplitude than that of NaCMC molecules which is also experimentally observed. Fig. 11a shows the combination of scatter plots with all translocations generated by NaCMC (blue circle, same plot as Fig 9d) and λ-DNA (red square, same plot as Fig 10d) using the same nanopore at an applied voltage of 10V. As expected, the translocation signatures of NaCMC and λ-DNA generate distinct current modulation amplitude and create two separate subgroups. From Fig. 11a, it can be assumed that translocations with differential amplitude more than 3nA (shown in green line) are most probably generated by λ-DNAs. As the two biomolecular translocations are distinguishable from each other, it is expected to be able to differentiate individual molecules based on their detection signatures if a mixture of them are going through the nanopore simultaneously.

To validate the claim, a mixture of NaCMC and λ-DNA molecules were loaded on the chip. As a voltage of 10V was applied across the nanopore and the outlet reservoir, molecular translocations were observed. Fig. 12b shows the scatter plot of all translocations generated by the mixture NaCMC and λ-DNA molecules. Again, two separate subgroups of translocation events with different differential current amplitude are seen (separation is shown in solid green line at 3nA) which is in very good agreement with the previous results. It can be concluded that translocations with differential amplitudes larger than 3nA are generated by λ-DNA, whereas translocations with differential amplitude smaller than 3nA are generated by NaCMC molecules. The experimental results clearly demonstrate the functionality of multiplexed biomolecular detection using the same nanopore device.
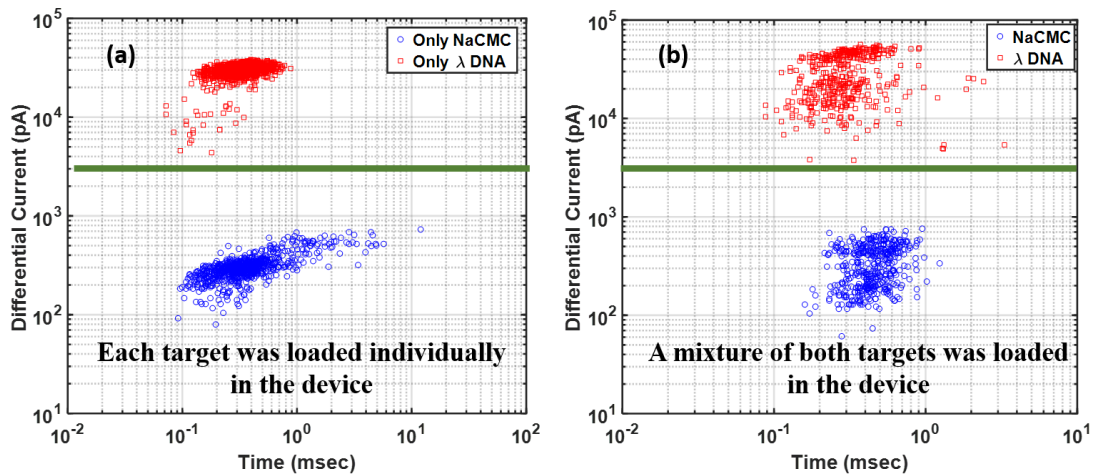
Figure 12. a. Combined scatter plot of dwell time vs. differential current when only NaCMC molecules (blue) translocate through the nanopore and when only λ-DNAs (red) translocate through the nanopore; b. Scatter plots of dwell time vs. differential current of translocation events generated when a mixture of NaCMC and λ-DNA molecules translocate through the nanopore simultaneously (Blue: Supposed NaCMC, Red: Supposed λ-DNA)

2.6 Feedback-gated cellulose detection

Previously in our group, we demonstrated biomolecules on-demand selective detection with the combination of solid-state nanopore and feedback electrical system.[30] The flowchart of the feedback controlled gating system is shown in Figure 13.
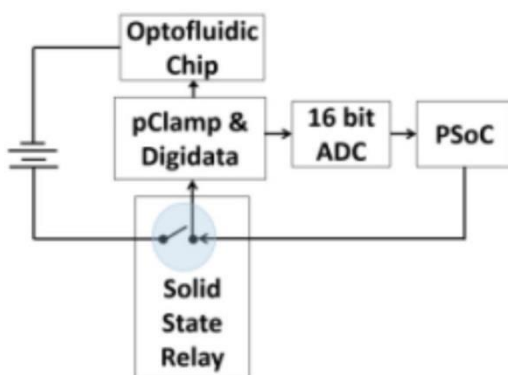
Figure 13. Flowchart of the feedback controlled gating system[30]

In regular experiments, we change the applied voltage manually through pClamp, and Digidata is directly connected to the electrodes in the nanopore reservoir and inlet reservoir. But if we want to stop or restart the translocation process by changing voltage manually, it will take a long time and result in getting unwanted translocation. So, in the feedback system, we use PSOC as the microcontroller to control the applied voltage across the nanopore and the inlet instead of direct applying voltage from Digidata. For regular nanopore detection experiments we just record the current signal in PC through AxoScope. But in this case, we also input the real-time current signal to PSOC as well as monitor and record the signal on PC. By loading codes for spike detecting, PSOC

can detect if there is a current signal spike or not. If there is a spike, the PSOC will automatically stop the applied voltage. So that only one molecule passes through the nanopore this time.

The capability of detecting cellulose has already been shown in 2.3. Here we show that the delivery of NaCMC through the nanopore can also be controlled using our feedback control system.

Figure 14 shows the data traces of NaCMC detection with feedback gating control circuit. We can see that in the inset (a) when one current peak created by one molecule translocation, the circuit detected this current change and firstly reset the detection voltage to zero (shown in the inset (b)) then the applied voltage becomes zero (shown in the inset (c)) so that no further NaCMC molecules will go through. Until manually reset or preset reset time, the applied voltage will keep as zero.
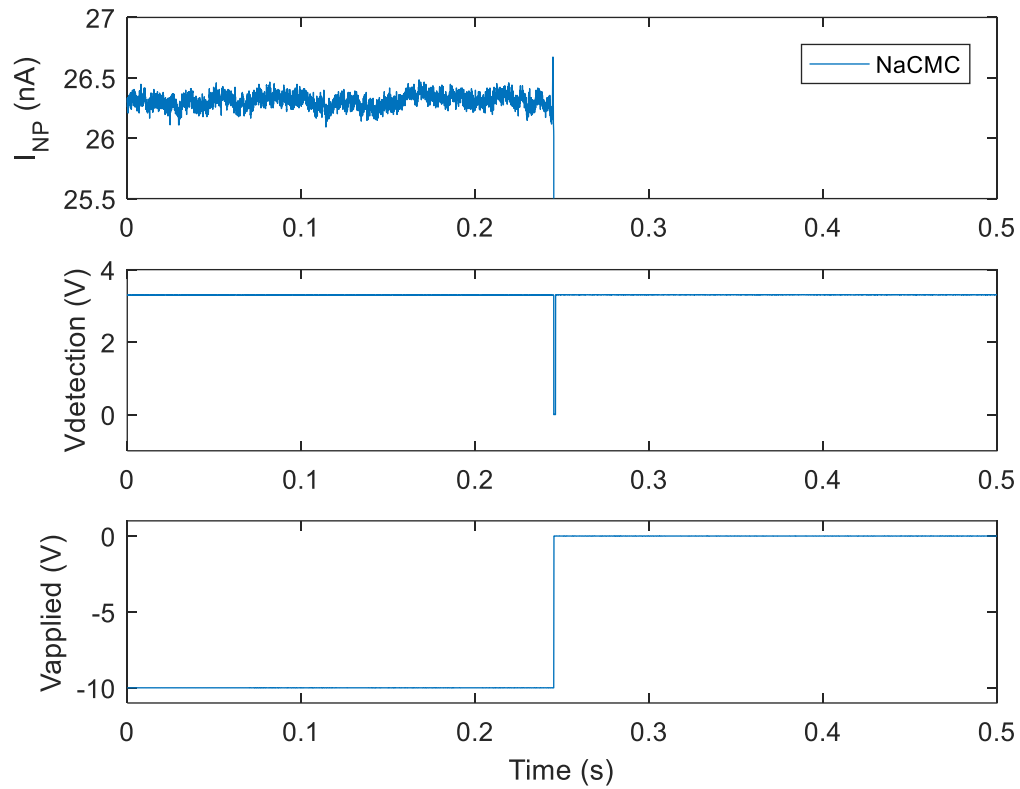
Figure 14. a. Current Trace of one NaCMC Translocation; b. Voltage trace of the detection signal; c. Voltage trace of the applied voltage

We can also change the number of current spikes to get the number of passing through the nanopore. Once the number reaches certain predetermined conditions, the circuit will automatically turn off the applied voltage to stop any further translocation events. We demonstrated that we could control the number of biomolecules passing through the nanopore on this platform.

2.7 Discussion and Summary

In this chapter, we discussed the new fabrication method of integrating micropores with microfluidic devices for the purpose of getting reproducible devices and controlled processes. Though the results of the fabrication are not as expected, which means the processes still need to be improved, with certain post-treatment on the current pre-fabricated membranes, we still got a thin and flat membrane on top of the fluid channel and drilled nanopore on this membrane. On this device, we successfully detected 100bp DNA Ladder, λ-DNA, and NaCMC. We also demonstrated multiplex detection by detecting NaCMC and λ-DNA in the mixture of them and distinguishing them based on the current spike patterns. Based on the feedback control system, we can deliver a certain number of NaCMC molecules through the nanopore.

3 Biomolecule detection with ion-beam sculpted nanopore

3.1 Method of shrinking pre-fabricated nanopore by ion beam deposition

As discussed in the previous chapter, we used the ion beam to drill a nanopore directly on the thin SiO_2 membrane. Due to the limitation of ions own size and focus quality, it is difficult to get a small nanopore. And because the SNR ratio can be increased by the decrease of the pore diameter[26], we are thinking to add some post-treatment steps to shrink the nanopore with direct ion beam drilling.

Liu et al, previously discussed different fabrication methods of the nanopore and their effect on the nanopore properties. [31] After direct drilling, we can either use an electron beam or ion beam to tune the pore size. Here we used the ion beam to shrink a nanopore on our microfluidic device. After direct drilling a nanopore, we can redeposit some materials on top of the pre-fabricated nanopore to shrink its size down. In details, we choose a square area which is much larger than nanopore, and the nanopore sits at the center of this square. Then we turn on the valve of silicon oxide gas, let the gas fill the chamber of SEM and then expose the square area we choose with ion beam for a short time to deposit some silicon oxide on the nanopore. The parameters we choose are described below: we deposition SiO_2 on a 1.5um square with a current of 1.5 pA for 10s.

Figure 9a is the SEM image of a nanopore with direct drilling. After one-time deposition, it shrinks, and the SEM image of ion sculpted pore is Figure 9b. From these two figures, we can clearly see that the diameter of nanopore reduces and from the

rough measurement we claimed that the diameter of the nanopore is shrunk from 20nm to 14nm.
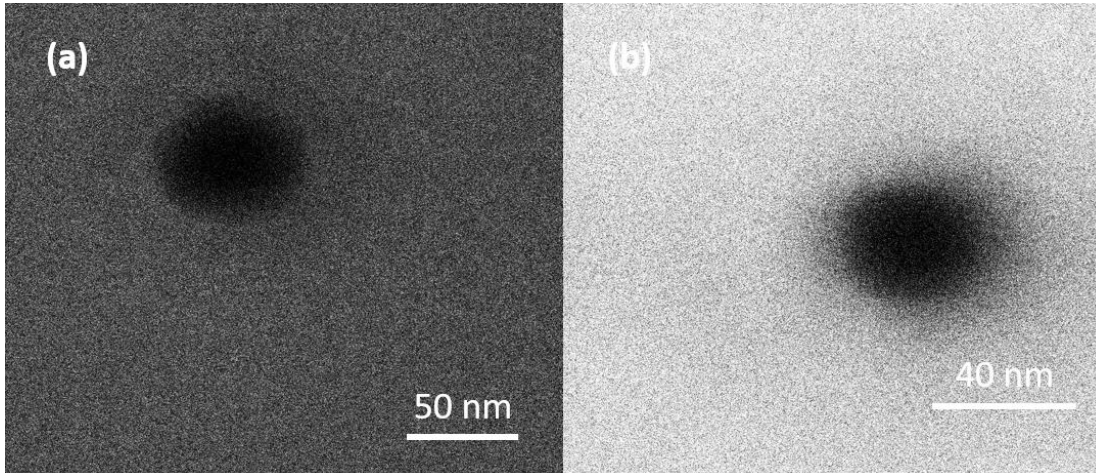
Figure 15. a. SEM image of a nanopore with FIB direct drilling; b. the nanopore after ion beam sculpted

3.2 Electrical properties test

Furthermore, we would like to investigate the difference in the electrical properties of the nanopore before and after ion beam deposition. Here we showed the characterization results of two important electrical properties of the nanopore. One is the IV curve. The current passing through the nanopore with the different applied voltage across the inlet and the nanopore when the chip is filled with certain buffer solution is recorded before plotting the IV curve. From the IV curve, we can know the current response at different applied voltage levels and roughly calculate the resistance of the whole path from the inlet to the nanopore.

We can also calculate the power spectrum of the baseline current. It shows the power distribution of signals in different frequencies. From the power spectrum of a trace of baseline, we can know the noise power level at different frequencies. Based on the power spectrum, we can investigate the possible sources of the electrical noise of the nanopore.

The results of the IV curve and power spectrum of the pre-fabricated nanopore and ion sculpted nanopore are shown below.

3.2.1 I-V Curves

The IV curves of the nanopore before and after shrinking are shown here. We can see that the baseline current decreased with the same applied voltage. The resistance of nanopore increases, which means the diameter of nanopore decreased. [32]
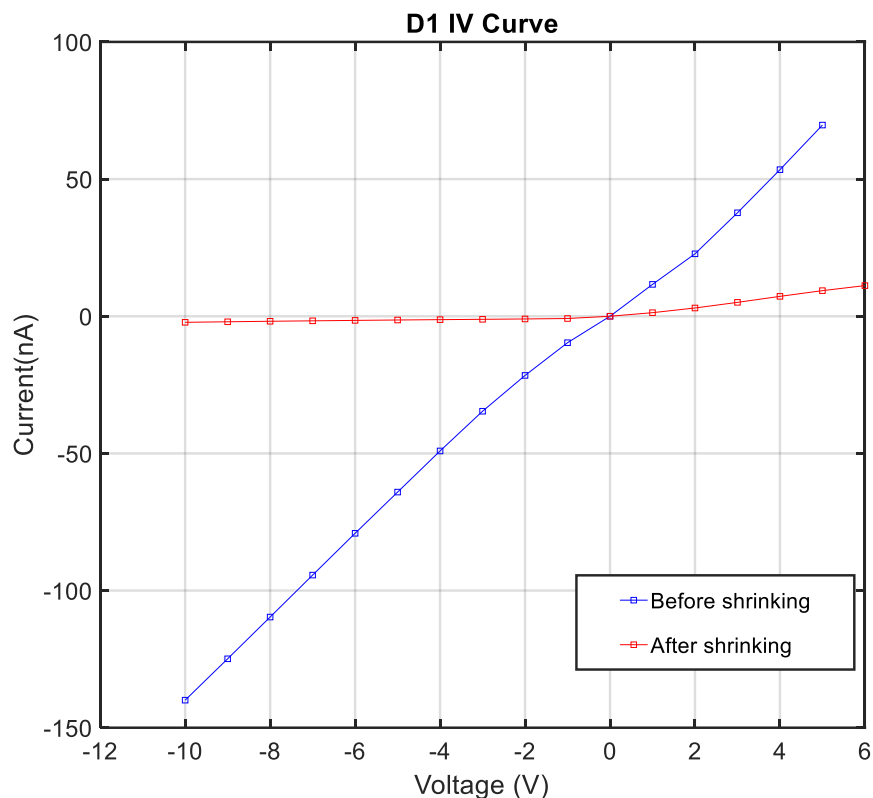
Figure 16. IV Curve of Nanopore on Chip No. D1: Blue: Nanopore Before Ion-sculpting Red: Nanopore After Ion-sculpting

3.2.2 Baseline power spectrum

The power spectra (generated by Clampfit, Molecular Device) of the baseline current from the nanopore before and after shrinking are shown here. From the graph, we can tell there may be a decrease of the noise of the nanopore after ion sculpting. That may indicate it is possible that the re-deposition step not only changes the diameter of the nanopore but also change the surface properties of the nanopore, which reduce the noise background. More research needs to be done to discuss this possibility further.
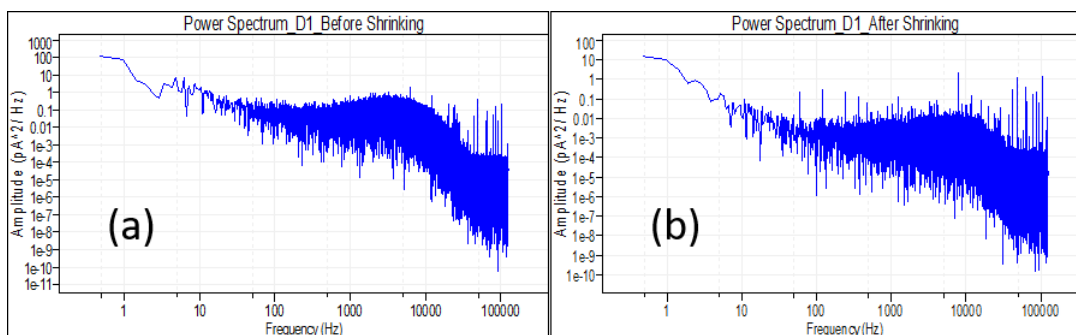
Figure 17. a. The power spectrum of the nanopore before shrinking based on a segment of baseline current with the applied voltage of 10V; b. The power spectrum of the nanopore after shrinking based on a segment of baseline current with the applied voltage of 10V

3.3 NaCMC detection on ion-beam sculpted nanopore

NaCMC has also been detected using this ion-beam sculpted nanopore. Current traces are shown in Fig. 9. We demonstrated that we are able to detect NaCMC using the ion sculpted nanopore. From the scatter plot of the preliminary results (Figure.9c), we can see there is some variation in the shapes of the current spikes. The reasons need to be investigated.
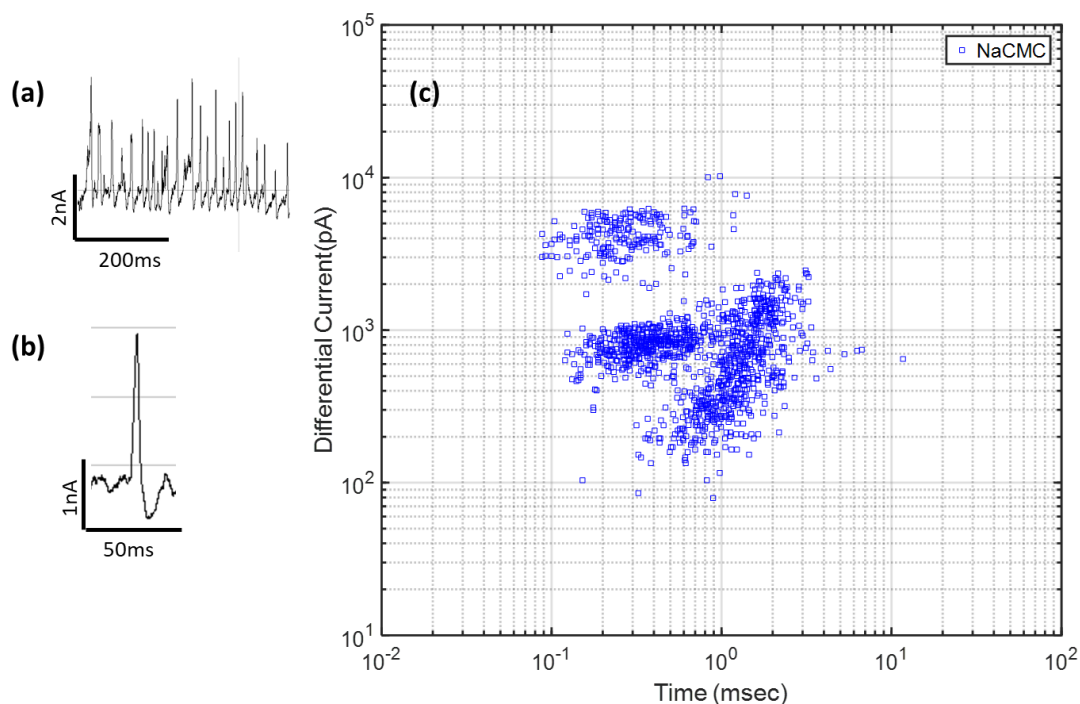
Figure 18. a. Current trace of NaCMC translocation events; b. Zoomed in single NaCMC translocation; c. Scatter plot of dwell time vs differential current of NaCMC translocations.

3.4 Discussion and Summary

To improve the sensitivity of the nanopore, we discussed the second step ion sculpting of the direct drilling. After successfully fabricating the ion-sculpted nanopore, we preliminary investigated some electrical properties of the ion-sculpted nanopore and performed the NaCMC detection on this nanopore. The results of this chapter are the beginning of further research on the performance of ion-sculpted nanopore.

31

4 Summary and Outlook

4.1 Summary

In this thesis, we demonstrated a new process of fabricating micropore on top of the microfluidic device using standard semiconductor fabrication processes. And the characterization of the device has been done, and post-treatment of thinning down the SiO_2 membrane has been done to improve the quality of nanopore on this new kind of microfluidic device. On this device, we demonstrated first detection of NaCMC with a nanopore. And based on this platform we also succeeded in detecting nucleic acid and detecting of both NaCMC and λ-DNA in a mixture of them and distinguish them from the scatter plot of the amplitude and duration time current spikes which are brought by the translocations of molecules. By combining the feedback control system with our platform, we also demonstrated controlled number delivery of NaCMC. To investigate the method of improving the nanopore quality more, we also shrank a nanopore using ion beam. We investigated the electronic properties of the nanopore with ion beam direct drilling and after ion beam sculpted and successfully detected NaCMC using this ion beam sculpted nanopore.

4.2 Outlook

This thesis is just the start of an investigation on the applications of this nanopore-microfluidic platform. There is still lots of work to do. Firstly, to expand the applications of our platform, more kinds of a mixture of different targets need to be detected on this platform. Second, we need to study more about the process of

micropore fabrication on the microfluidic device and try to improve the process to increase the micropore quality. For studying ion-sculpted nanopore, if we can make both the pre-fabricated nanopore and ion-beam sculpted nanopore be sensitive to same biomolecules, we can have a more direct comparison on the nanopore-shape dependence of current spike shape. Also, more theoretical work and simulation need to be done to find the reasons for the difference in electrical properties of the nanopore before and after shrinking.

Bibliography

1.   Siwy, Z. S. Ion-current rectification in nanopores and nanotubes with broken symmetry. *Adv. Funct. Mater.* **16**, 735–746 (2006).

2.   Smeets, R. M. M., Dekker, N. H. & Dekker, C. Low-frequency noise in solid-state nanopores. *Nanotechnology* **20**, 95501 (2009).

3.   Zhang, B., Zhang, Y. & White, H. S. The Nanopore Electrode. **76**, 6229–6238 (2004).

4.   Chen, P. *et al.* Probing single DNA molecule transport using fabricated nanopores. *Nano Lett.* **4**, 2293–2298 (2004).

5.   Stoddart, D., Heron, A. J., Mikhailova, E., Maglia, G. & Bayley, H. Single-nucleotide discrimination in immobilized DNA oligonucleotides with a biological nanopore. *Proc. Natl. Acad. Sci.* **106**, 7702–7707 (2009).

6.   Purnell, R. F., Mehta, K. K. & Schmidt, J. J. Nucleotide identification and orientation discrimination of DNA homopolymers immobilized in a protein nanopore. *Nano Lett.* **8**, 3029–3034 (2008).

7.   Jain, M., Olsen, H. E., Paten, B. & Akeson, M. The Oxford Nanopore MinION: Delivery of nanopore sequencing to the genomics community. *Genome Biol.* **17**, 1–11 (2016).

8.   Ying, Y. L., Cao, C. & Long, Y. T. Single molecule analysis by biological nanopore sensors. *Analyst* **139**, 3826–3835 (2014).

9. Storm, A. J., Chen, J. H., Ling, X. S., Zandbergen, H. W. & Dekker, C. Fabrication of solid-state nanopores with single-nanometre precision. *Nat. Mater.* **2**, 537–540 (2003).

10. Kasianowicz, J. J., Brandin, E., Branton, D. & Deamer, D. W. Characterization of individual polynucleotide molecules using a membrane channel. *Proc. Natl. Acad. Sci. U. S. A.* **93**, 13770–3 (1996).

11. Butler, T. Z., Pavlenok, M., Derrington, I. M., Niederweis, M. & Gundlach, J. H. Single-molecule DNA detection with an engineered MspA protein nanopore. *Proc. Natl. Acad. Sci.* **105**, 20647–20652 (2008).

12. Butler, T. Z., Gundlach, J. H. & Troll, M. A. Determination of RNA Orientation during Translocation through a Biological Nanopore. *Biophys. J.* **90**, 190–199 (2006).

13. Dekker, C., Article, R. & Dekker, C. Solid-state nanopores. *Nat. Nanotechnol.* **2**, 209–215 (2007).

14. Park, S. R., Peng, H. & Ling, X. S. Fabrication of nanopores in silicon chips using feedback chemical etching. *Small* **3**, 116–119 (2007).

15. Li, J. *et al.* Ion-beam sculpting at nanometre length scales. *Nature* **412**, 166–169 (2001).

16. Venkatesan, B. M. *et al.* DNA Sensors: Highly Sensitive, Mechanically Stable Nanopore Sensors for DNA Analysis (Adv. Mater. 27/2009). *Adv. Mater.* **21**,

n/a-n/a (2009).

17.   Garaj, S. *et al.* Graphene as a subnanometre trans-electrode membrane. *Nature*
       467, 190–193 (2010).

18.   Schneider, G. F. *et al.* DNA translocation through graphene nanopores. *Nano
       Lett.* **10**, 3163–3167 (2010).

19.   Merchant, C. A. *et al.* DNA translocation through graphene nanopores. *Nano
       Lett.* **10**, 2915–2921 (2010).

20.   Whitesides, G. M. The origins and the future of microfluidics. **442**, (2006).

21.   Sia, S. K. & Whitesides, G. M. Microfluidic devices fabricated in
       poly(dimethylsiloxane) for biological studies. *Electrophoresis* **24**, 3563–3576
       (2003).

22.   Yager, P. *et al.* Microfluidic diagnostic technologies for global public health.
       Nature **442**, 412–8 (2006).

23.   Jain, T., Guerrero, R. J. S., Aguilar, C. A. & Karnik, R. Integration of solid-
       state nanopores in microfluidic networks via transfer printing of suspended
       membranes. *Anal. Chem.* **85**, 3871–3878 (2013).

24.   Rudenko, M. I. *et al.* Controlled gating and electrical detection of single 50S
       ribosomal subunits through a solid-state nanopore in a microfluidic chip.
       Biosens. Bioelectron. **29**, 34–39 (2011).

25.   Liu, S. *et al.* Correlated Electrical and Optical Analysis of Single

Nanoparticles and Biomolecules on a Nanopore-Gated Opto fl uidic Chip. *Nano Lett.* (2015). doi:10.1021/nl502400x

26. Lee, K. *et al.* Enhancing the sensitivity of DNA detection by structurally modified solid-state nanopore. *Nanoscale* **9**, 18012–18021 (2017).

27. Griffith, J. D., Willcox, S., Powers, D. W., Nelson, R. & Baxter, B. K. Discovery of Abundant Cellulose Microfibers Encased in 250 Ma Permian Halite: A Macromolecular Target in the Search for Life on Other Planets. *Astrobiology* **8**, 215–228 (2008).

28. Lopez, C. G., Rogers, S. E., Colby, R. H., Graham, P. & Cabral, J. T. Structure of sodium carboxymethyl cellulose aqueous solutions: A SANS and rheology study. *J. Polym. Sci. Part B Polym. Phys.* **53**, 492–501 (2015).

29. Yang, C., Moses, D. & Heeger, A. J. Base-Pair Stacking in Oriented Films of DNA–Surfactant Complex. *Adv. Mater.* **15**, 1364–1367 (2003).

30. Rahman, M., Harrington, M., Stott, M. A., Hawkins, A. R. & Schmidt, H. Single Particle Fluorescence Analysis on Demand on Electro-Optofluidic Chip with Gated Particle Delivery. in *Conference on Lasers and Electro-Optics* SM2C.5 (Optical Society of America, 2017). doi:10.1364/CLEO_SI.2017.SM2C.5

31. Liu, S., Yuzvinsky, T. D. & Schmidt, H. Effect of fabrication-dependent shape and composition of solid-state nanopores on single nanoparticle detection. *ACS*

Nano **7**, 5621–5627 (2013).

32.   Smeets, R. M. M. *et al.* Salt dependence of ion transport and DMA

translocation through solid-state nanopores. *Nano Lett.* **6**, 89–95 (2006).